Nonlinear elasticity in III-N compounds: *Ab initio* calculations

S. P. Łepkowski
Unipress—Institute of High Pressure Physics, Polish Academy of Sciences, ulica Sokołowska 29, 01-142 Warszawa, Poland

J. A. Majewski
Institute of Theoretical Physics, Faculty of Physics, Warsaw University, ulica Hoża 69, 00-681 Warszawa, Poland

G. Jurczak
Institute of Fundamental Technological Research, Polish Academy of Sciences, ulica Świętokrzyska 21, 00-049 Warszawa, Poland
(Received 26 August 2005; published 1 December 2005)

We have studied the nonlinear elasticity effects in zinc-blende and wurtzite crystallographic phases of III-N compounds. Particularly, we have determined the pressure dependences of elastic constants in InN, GaN, and AlN by performing *ab initio* calculations in the framework of plane-wave pseudopotential implementation of the density-functional theory. The calculations have been performed employing two exchange-correlation functionals, one within the local density approximation and the other within the generalized gradient approximation. We have found that C_{11}, C_{12} in zinc-blende nitrides and C_{11}, C_{12}, C_{13}, C_{33} in wurtzite nitrides depend significantly on hydrostatic pressure. Much weaker dependence on pressure has been observed for C_{44} elastic constant in both zinc-blende and wurtzite phases. Further, we have examined the influence of pressure dependence of elastic constants on the pressure coefficient of light emission, dE_E/dP, in wurtzite InGaN/GaN and GaN/AlGaN quantum wells. We have shown that the pressure dependence of elastic constants leads to a significant reduction of dE_E/dP in nitride quantum wells. Finally, we have considered the influence of nonlinear elasticity of III-N compounds on the properties of hexagonal nitride quantum dots (QDs). For typical wurtzite GaN/AlN QDs, we have shown that taking into account pressure dependence of elastic constants results in the decrease of volumetric strain in the QD region by about 7%. Simultaneously, the average z component of the piezoelectric polarization in the QDs increases by 0.1 MV/cm compared to the case when linear elastic theory is used. Both effects, i.e., decrease of volumetric strain as well as increase of piezoelectric field, decrease the band-to-band transition energies in the QDs.

DOI: 10.1103/PhysRevB.72.245201 PACS number(s): 78.67.De, 62.20.Dc, 62.50.+p, 78.67.Hc

I. INTRODUCTION

The electronic and optical properties of semiconductor heterostructures depend crucially on the strain arising from the lattice mismatch. Commonly, the strain effects in quantum structures, i.e., quantum wells (QWs), wires, or dots (QDs), are described within the standard elasticity theory, in which the deformation energy is described by terms quadratic in the strain tensor components and elastic constants are independent of the strain (so-called linear theory). Nevertheless, there are circumstances where this simple approach is not sufficient.

Nonlinear elastic properties of GaAs and InAs have recently attracted significant attention. First, Frogley *et al.* proposed that pressure dependences of elastic constants in GaAs and InAs are required to explain anomalously the small pressure coefficient of band gap (dE_G/dP) in strained InGaAs layers.[1] They showed that the main contribution, responsible for drastic reduction of dE_G/dP in biaxial strained layers of InGaAs, came from the pressure dependence of a two-dimensional Poisson's ratio, $\nu_{2D}(P)$, defined for zinc-blende structure as $2C_{12}/C_{11}$. Second, Ellaway *et al.* calculated pressure dependences of elastic constants for InAs and discussed their influence on the properties of InAs/GaAs QDs.[2] They noticed that the hydrostatic strain component in the InAs/GaAs QDs is significantly overestimated by calculations based on the linear theory of elasticity. Taking into account the pressure dependence of elastic constants reduces the hydrostatic strain by about 16%.[2] Recently, it has also been shown that pressure dependences of elastic constants in GaAs and InAs are decisive to determine the pressure coefficients of the light emission (dE_E/dP) in InAs/GaAs QDs.[3,4]

For the case of wurtzite III-N compounds, the nonlinear elasticity effects have not been systematically studied yet. A pioneering paper in this field was published by Kato and Hama who calculated the pressure dependence of the elastic stiffness tensor for wurtzite AlN.[5] Later on, Vaschenko *et al.* used these results to estimate the influence of the nonlinear elasticity on dE_E/dP in hexagonal AlGaN/GaN QWs.[6] Recently, we have investigated the pressure dependences of elastic constants, in zinc-blende InN and GaN.[7] We have shown that one has to take the effects of nonlinear elasticity into account in order to determine dE_E/dP in cubic InGaN/GaN QWs.[7]

In this work, we focus on the nonlinear elasticity effects in group III nitrides crystallizing in wurtzite structure. Particularly, we have determined the pressure dependences of elastic constants in wurtzite InN, GaN, and AlN by performing *ab initio* calculations in the framework of plane-wave pseudo-potential implementation of the density-functional theory.[8,9] We have used two approximations to the exchange-correlation functionals, the standard local density approxima-

 ©2005 The American Physical Society

tion (LDA) and the generalized gradient approximation (GGA), in the present calculations. This allows us to judge the accuracy of such calculations. The paper is organized as follows. In Sec. II, we discuss, first, the computational procedure employed to determine the pressure dependence of the elastic constants. Next, we present results for the wurtzite phase of bulk nitrides, discuss the pressure dependence of Poisson coefficients, and finally provide comparison of the pressure dependence of elastic constants in zinc-blende and wurtzite crystallographic phases of nitrides. We illustrate the importance of the pressure dependence of the elastic constants discussing two systems, nitride heterostructures and quantum dots, in Secs. III and IV. The pressure coefficient of light emission dE_E/dP in wurtzite InGaN/GaN and GaN/AlGaN QWs is discussed in Sec. III, whereas the elastic, piezoelectric, and optical properties of wurtzite GaN/AlN quantum dots are discussed in Sec. IV. Finally we conclude the paper in Sec. V.

II. PRESSURE-DEPENDENT ELASTIC CONSTANTS IN BULK NITRIDES

A. Computational procedure

The pressure dependence of the elastic constants is customarily defined as

$$C_{\alpha\beta}(P) = \frac{1}{V_P}\frac{\partial^2 E_{tot}(V_P)}{\partial\varepsilon_\alpha \partial\varepsilon_\beta}, \tag{1}$$

where $E_{tot}(V_P)$ is the total energy per unit cell, V_P is the unit cell volume at given pressure P, which is found by solving $P=-\partial E_{tot}/\partial V$, and ε_α, ε_β are the elements of the infinitesimal strain tensor.[10] For simplicity, we use the Voigt notation hereafter. To determine $C_{\alpha\beta}(P)$ [where $(\alpha\beta)=(11),(12),(13),(33),(44)$] for wurtzite GaN, InN, and AlN, we have carried out the total energy calculations based on a plane-wave pseudo-potential implementation of the density-functional theory.[8] The numerical computations have been performed with the VASP package.[9]

The calculations of the pressure dependence of the elastic constants are performed in two steps. In the first step, we calculate the total energy of the bulk wurtzite crystal as a function of the unit cell volume. Then, using the definition of pressure, $P=-\partial E_{tot}/\partial V$, one can find the unit cell volume corresponding to the certain value of the external pressure P. In this step, for a given unit cell volume, the unit cell shape (i.e., c/a ratio) and unit cell geometry (i.e., internal parameter u) are optimized. The obtained values of c/a and u as a function of the hydrostatic pressure are depicted in Figs. 1(a) and 1(b). As can be seen from these figures, one can correlate the magnitude of changes in c/a and u under the hydrostatic pressure with deviations of the nitride structures from "ideal" wurtzite. The weakest dependences of c/a and u on the hydrostatic pressure are obtained for GaN, which possesses the smallest deviation of c/a from the ideal value 1.633. The strongest dependences c/a and u on the hydrostatic pressure are observed for AlN, which has the largest deviation of c/a from the ideal value.

In the second step, the unit cell at certain pressure is subject to test distortions. The magnitude of the components of the strain tensor that characterizes the test distortion ($\hat{\varepsilon}_{\alpha\beta}$) is much smaller in comparison to the hydrostatic strain component corresponding to the value of applied pressure P. The elastic energy of the deformed lattice at hydrostatic pressure P, $E_{elst}(P)$, is defined exactly in the same way as at zero (ambient) pressure, namely, as the contribution to the total energy with terms quadratic in the components of the strain tensor ($\hat{\varepsilon}_{\alpha,\beta}$). Of course, the elastic energy is now characterized by the elastic constants that are dependent on the hydrostatic pressure. To determine the pressure-dependent elastic constants, the deformation energies $E_{elst}(P)$ have been computed for a series of test displacements in the range of -1% to 1% and have been fitted by the second-order polynomials to the expressions from the elasticity theory. The test distortions applied in the present calculations are identical to those used previously by Wright[11] and are listed in Table I. When the test distortions are applied, positions of atoms in the unit cell have been obtained by allowing additional atomic relaxation and modification of the unit cell shape.

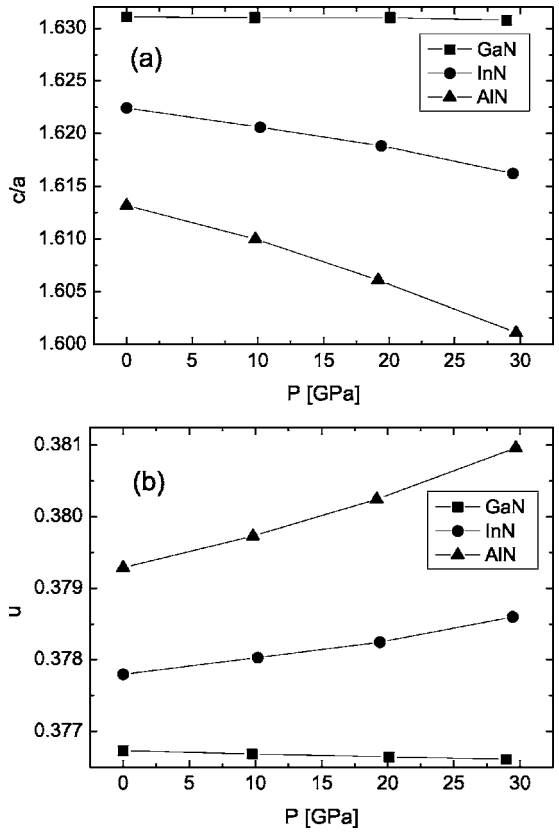

FIG. 1. (a) The axial ratio, c/a, and (b) the internal parameter, u, of the wurtzite structure as a function of the hydrostatic pressure for GaN, InN, and AlN. Solid lines are added to guide the eye.

The total energy calculations have been performed using two different approximations to the exchange-correlation functionals, namely, the local density approximation (LDA) with the Ceperley-Alder correlation functional as parametrized by Perdew and Zunger,[12] and the generalized gradient approximation (GGA) within the and Perdew-Wang functional.[13] In both cases the projector augmented wave pseudopotentials have been used.[14] The semi-core Ga $3d$ and In $4d$ states have been treated as valence electrons. Brillouin-zone

TABLE I. Test distortions and corresponding expressions for elastic energies used to calculate pressure-dependent elastic constants in wurtzite nitrides.

$\hat{\varepsilon}_{\alpha\beta}=(\varepsilon_{xx},\varepsilon_{yy},\varepsilon_{zz},\varepsilon_{zx},\varepsilon_{zy},\varepsilon_{yx},)$	$E_{elst}(P)$
$(\delta,\delta,0,0,0,0)$	$[C_{11}(P)+C_{12}(P)]\delta^2$
$(\delta,\delta,-2\delta,0,0,0)$	$[C_{11}(P)+C_{12}(P)-4C_{13}(P)+2C_{33}(P)]\delta^2$
$(0,0,\delta,0,0,0)$	$C_{33}(P)\delta^2/2$
$(0,0,0,0,0,\delta/2)$	$[C_{11}(P)-C_{12}(P)]\delta^2/4$
$(0,0,0,\delta/2,\delta/2,0)$	$C_{44}(P)\delta^2$

integrations have been performed using a $9\times9\times7$ Monkhorst-Pack k-space grid. The kinetic energy cutoff for the plane-wave expansion of crystalline wave functions has been chosen to be equal to 800 eV.

B. Nonlinear effects in wurtzite structure

In Figs. 2(a)–2(c), we present the pressure dependence of the elastic constants, $C_{11}(P)$, $C_{12}(P)$, $C_{13}(P)$, $C_{33}(P)$ and $C_{44}(P)$, obtained for wurtzite GaN, InN, and AlN using both LDA and GGA in the range of hydrostatic pressure 0–30 GPa. One can notice that the elastic constants C_{11}, C_{12}, C_{13}, C_{33} show considerable increase with pressure, whereas C_{44} exhibits much weaker dependence on pressure. Since dependence of the elastic constants on pressure $C_{\alpha\beta}(P)$ shows slightly sublinear character in the investigated range of hydrostatic pressures, we describe $C_{\alpha\beta}(P)$ using second-order polynomials in P:

$$C_{\alpha\beta}(P) = C_{\alpha\beta} + C_{\alpha\beta}{}' \cdot P + \tfrac{1}{2}C_{\alpha\beta}{}'' \cdot P^2.$$

The expansion coefficients, $C_{\alpha\beta}$, $C_{\alpha\beta}{}'$, and $C_{\alpha\beta}{}''$, together with the values of bulk modulus, B_0, and its pressure derivative B_0', have been collected for wurtzite AlN, GaN, and InN in Table II. For wurtzite systems, B_0 and B_0' can be expressed in terms of the zero pressure elastic constants $C_{\alpha\beta}$ and linear coefficients $C_{\alpha\beta}{}'$ as follows:

$$B_0 = \frac{C_{33}(C_{11}+C_{12}) - 2(C_{13})^2}{C_{11}+C_{12}-4C_{13}+2C_{33}}, \tag{2}$$

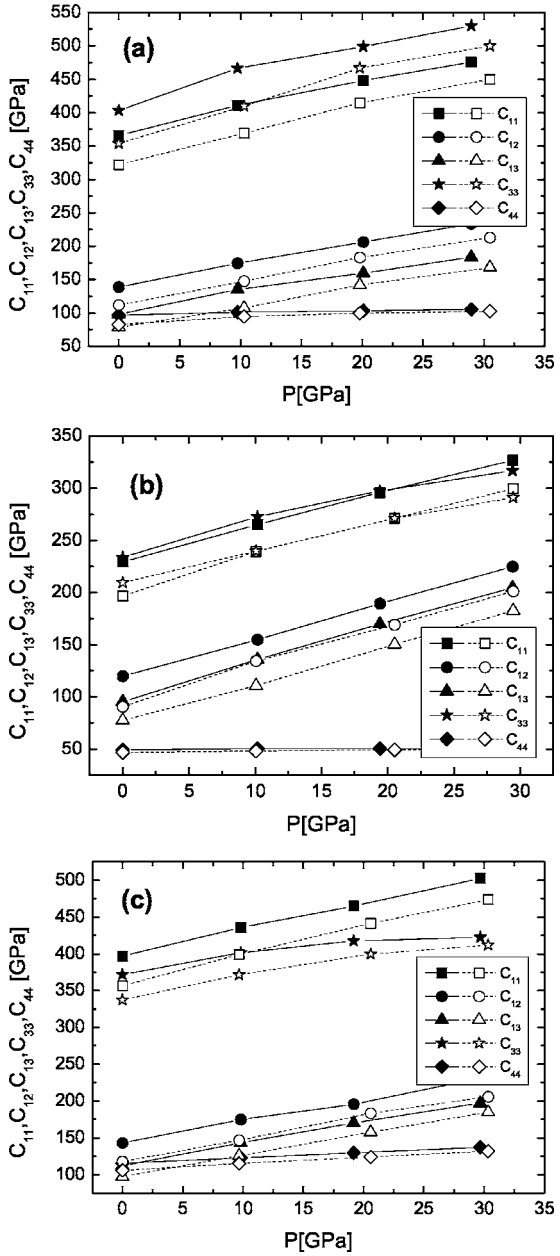

FIG. 2. Elastic constants of wurtzite structure as a function of the hydrostatic pressure for GaN (a), InN (b), and AlN (c). Full and empty symbols represent values obtained using LDA-DFT and GGA-DFT methods, respectively. Solid and dashed lines are added to guide the eye.

$$B_0' = \frac{C_{33}'(C_{11}+C_{12}) + C_{33}(C_{11}'+C_{12}') - 4C_{13}C_{13}' - B_0(C_{11}'+C_{12}'-4C_{13}'+2C_{33}')}{C_{11}+C_{12}-4C_{13}+2C_{33}}. \tag{3}$$

For comparison, in Table II we have also included the values of $C_{\alpha\beta}$, B_0, and B_0' that have been previously obtained in various calculations. One can see that the values of elastic constants $C_{\alpha\beta}$ and bulk moduli B_0 obtained in the present calculations are rather close to the results reported in Refs. 11 and 15. The values of B_0' are also in good agreement with

TABLE II. Second-order polynomials obtained from the fit to numerically calculated pressure-dependent elastic constants, $C_{\alpha\beta}(P)$, for wurtzite nitrides in the pressure range of 0–30 GPa. The values of bulk modulus, B_0, and its pressure derivative, B_0', are also given. For comparison, the results of other authors are included in the table.

	LDA—present results	GGA—present results	LDA[a,b]	GGA[d]
w-GaN				
C_{11}	$366+4.88P-0.038P^2$	$322+5.23P-0.033P^2$	367[a]	
C_{12}	$139+3.69P-0.015P^2$	$112+3.90P-0.018P^2$	135[a]	
C_{13}	$98+3.75P-0.029P^2$	$79+3.27P-0.001P^2$	103[a]	68
C_{33}	$403+6.54P-0.079P^2$	$354+6.7P-0.059P^2$	405[a]	354
C_{44}	$97+0.49P-0.007P^2$	$83+1.33P-0.023P^2$	95[a]	
B_0	200.6	170.9	202[a]	
B_0'	4.30	4.23	4.5[b]	
w-InN				
C_{11}	$229+3.66P-0.012P^2$	$197+4.29P-0.028P^2$	223[a]	
C_{12}	$120+3.51P+0.002P^2$	$90+4.32P-0.021P^2$	115[a]	
C_{13}	$95+4.11P-0.014P^2$	$78+3.36P-0.008P^2$	92[a]	70
C_{33}	$234+4.26P-0.049P^2$	$210+3.32P-0.018P^2$	224[a]	205
C_{44}	$49+0.15P-0.004P^2$	$47+0.17P-0.003P^2$	48[a]	
B_0	145.6	121.8	141[a]	
B_0'	3.92	3.78	3.4[b]	
w-AlN				
C_{11}	$397+3.78P-0.009P^2$	$356+4.65P-0.026P^2$	$380+3.96P-0.05P^2$,[c] 396[a]	
C_{12}	$143+2.78P+0.004P^2$	$118+3.45P-0.016P^2$	$114+6.83P-0.15P^2$,[c] 137[a]	
C_{13}	$112+3.34P-0.016P^2$	$97+3.02P-0.004P^2$	$127+2.89P-0.08P^2$,[c] 108[a]	94
C_{33}	$372+3.65P-0.066P^2$	$337+4.15P-0.055P^2$	$382-0.001P+0.06P^2$,[c] 373[a]	377
C_{44}	$116+0.75P-0.0008P^2$	$106+0.99P-0.005P^2$	$109-0.96P+0.04P^2$,[c] 116[a]	
B_0	210.3	185.4	207[a]	
B_0'	3.36	3.58	3.8[b]	

[a]Reference 11.
[b]Reference 16.
[c]Reference 5.
[d]Reference 15.

results from Ref. 16. We confirm the observation from Ref. 15 that $C_{\alpha\beta}$ obtained by the GGA-DFT are smaller than those calculated using the LDA-DFT. Looking at the linear terms in parabolic approximations of $C_{\alpha\beta}(P)$, one can observe that generally the increase of $C_{\alpha\beta}(P)$ with pressure is similar for all three bulks, GaN, AlN, and InN. Interestingly, the linear terms in $C_{\alpha\beta}(P)$ are usually higher for results obtained using the GGA-DFT than the LDA-DFT (C_{13}' for w-InN and w-AlN, and C_{33}' for w-InN are the exceptions). However, the differences in B_0' are rather small, which suggests that, in general, the nonlinear compressibility of the lattice is similar for both the LDA-DFT and the GGA-DFT. Comparing the values of $C_{\alpha\beta}{}'$ obtained by us for w-AlN with those published in Ref. 5, one can observe that quantitative agreement is reached for C_{11}' and C_{13}'. The most significant difference is in C_{33}' which according to Ref. 5 is practically negligible. Our calculations do not confirm this finding. Moreover, we obtain large values of C_{33}' also for GaN and InN, which raises a question about where the small value of C_{33}' obtained in Ref. 5 comes from. The quadratic terms in the parabolic approximations of $C_{\alpha\beta}(P)$ are usually rather small and negative [as a result of the small sublinear character of calculated $C_{\alpha\beta}(P)$] and will be neglected in further discussion.

C. Comparison of wurtzite with zinc-blende

In this section we compare the nonlinear elastic properties of zinc-blende and wurtzite GaN, AlN, and InN. We have calculated $C_{\alpha\beta,c}(P)(\alpha\beta)=(11),(12),(44)$ for the zinc-blende nitrides using essentially the identical procedure as the one described for wurtzite structures above. Hereafter the subscript "c" is used to indicate the values for cubic (zinc-blende) phase.

1. Results of ab initio calculations

For zinc-blende, we have used the following three test distortions with strain tensor components $\varepsilon_1,\ldots,\varepsilon_6$ defined as $(0,0,\delta,0,0,0)$, $(\delta,\delta,-2\delta,0,0,0)$, and $(0,0,0,0,0,\delta)$,

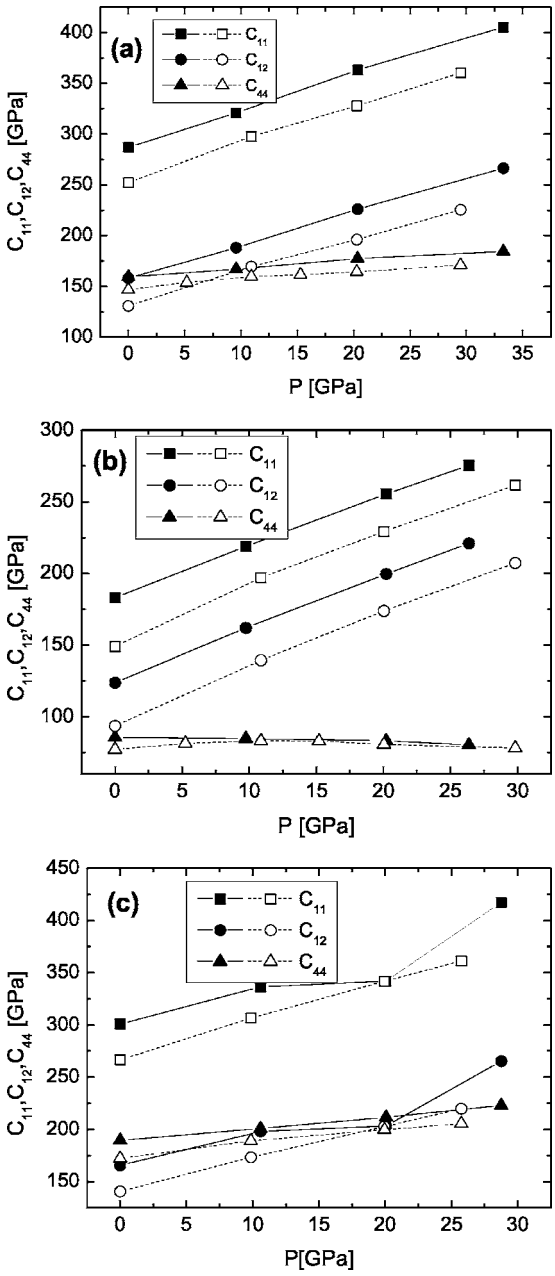

FIG. 3. Elastic constants of zinc-blende structure as a function of the hydrostatic pressure for GaN (a), InN (b), and AlN (c). Full and empty symbols represent values obtained using LDA-DFT and GGA-DFT methods, respectively. Solid and dashed lines are added to guide the eye.

which apparently differ from distortions used for wurtzite phase. The pressure-dependent elastic constants $C_{11,c}(P)$, $C_{12,c}(P)$, and $C_{44,c}(P)$ calculated for cubic, GaN, InN, and AlN are depicted in Figs. 3(a)–3(c). Both the LDA and GGA results for hydrostatic pressure in the range of 0–30 GPa are presented.[17] From Fig. 3, one can notice that $C_{11,c}(P)$ and $C_{12,c}(P)$ increase with pressure more significantly than $C_{44,c}(P)$. This weak dependence of $C_{44,c}(P)$ on hydrostatic pressure is then a unique feature of wurtzite and zinc-blende nitrides. Note that small variation of $C_{44,c}(P)$ with pressure P was also reported previously for zinc-blende InAs.[2]

As in the case of wurtzite bulks, we have fitted the $C_{\alpha\beta,c}(P)$ using second-order polynomials and results have been collected in Table III, together with the values of bulk modulus, $B_{0,c}=(C_{11,c}+2C_{12,c})/3$, and its pressure derivative $B'_c=(C'_{11,c}+2C'_{12,c})/3$. For comparison, we have also included values of $C_{\alpha\beta,c}$, $B_{0,c}$ and B'_{0c} taken from the literature.[11,16,18] Again, our $C_{\alpha\beta,c}$ and $B_{0,c}$ obtained by LDA-DFT are rather close to those reported in Ref. 11. Reasonable agreement with previous calculations is also observed for B'_c. Similarly to wurtzite phase, $C_{\alpha\beta,c}$ obtained by the GGA-DFT are smaller than those calculated using the LDA-DFT, whereas the coefficients $C'_{\alpha\beta,c}$ show opposite tendency. The quadratic terms in $C_{\alpha\beta,c}(P)$ are small and negative, as it was observed for wurtzite nitrides.

2. Nonlinear effects in wurtzite phase obtained from Martin's transformation

It is possible to obtain elastic constants of wurtzite material from the zinc-blende ones applying the so-called Martin's transformation.[19] The specific expressions for this relation have been listed in Ref. 11. These expressions lead to an approximate, albeit very reasonable, estimation of the elastic constants in wurtzite structure, provided the constants for zinc-blende phase are known.

It is interesting whether the pressure-dependent elastic constants of the wurtzite phase might also be reasonably approximated by Martin's transformation through the pressure-dependent elastic constants of the cubic phase. Simple algebra shows that the linear coefficients $C'_{\alpha\beta,M}$ in the wurtzite phase, as obtained from Martin's transformation, read

$$C'_{11,M}=\frac{1}{6}(3C'_{11,c}+3C'_{12,c}+6C'_{44,c})-\frac{1}{3}\frac{(C_{11,c}-C_{12,c}-2C_{44,c})(C'_{11,c}-C'_{12,c}-2C'_{44,c})}{(C_{11,c}-C_{12,c}+C_{44,c})}+\frac{1}{6}\frac{(C_{11,c}-C_{12,c}-2C_{44,c})^2(C'_{11,c}-C'_{12,c}+C'_{44,c})}{(C_{11,c}-C_{12,c}+C_{44,c})^2}, \tag{4}$$

$$C'_{12,M}=\frac{1}{6}(C'_{11,c}+5C'_{12,c}-2'C_{44,c})+\frac{1}{3}\frac{(C_{11,c}-C_{12,c}-2C_{44,c})(C'_{11,c}-C'_{12,c}-2C'_{44,c})}{(C_{11,c}-C_{12,c}+C_{44,c})}-\frac{1}{6}\frac{(C_{11,c}-C_{12,c}-2C_{44,c})^2(C'_{11,c}-C'_{12,c}+C'_{44,c})}{(C_{11,c}-C_{12,c}+C_{44,c})^2}, \tag{5}$$

$$C'_{13,M}=\tfrac{1}{6}(2C'_{11,c}+4C'_{12,c}-4C'_{44,c}), \tag{6}$$

$$C'_{33,M}=\tfrac{1}{6}(2C'_{11,c}+4C'_{12,c}+8C'_{44,c}), \tag{7}$$

TABLE III. Second-order polynomials obtained from the fit to numerically calculated pressure dependent elastic constants, $C_{\alpha\beta}(P)$, for zinc-blende crystallographic phase of nitrides in the range of pressures 0–30 GPa. The values of bulk modulus, B_0, and its pressure derivative, B_0', are also given. For comparison, the results of other authors are included in the table.

	LDA—present results	GGA—present results	LDA[a–c]
c-GaN			
$C_{11,c}$	$287+3.88P-0.009P^2$	$252+4.17P-0.019P^2$	293[a]
$C_{12,c}$	$158+3.33P-0.001P^2$	$131+3.50P-0.011P^2$	159[a]
$C_{44,c}$	$159+1.02P-0.007P^2$	$146+1.12P-0.012P^2$	155[a]
B_0	201	171.3	203.7[a]
B_0'	3.51	3.72	3.9,[b] 4.6[c]
c-InN			
$C_{11,c}$	$183+3.81P-0.011P^2$	$149+4.58P-0.029P^2$	187[a]
$C_{12,c}$	$124+4.01P+0.013P^2$	$94+4.37P+0.020P^2$	125[a]
$C_{44,c}$	$86+0.05P-0.009P^2$	$77+0.66P-0.023P^2$	86[a]
B_0	143.7	112.3	145.7[a]
B_0'	3.94	4.44	4.4,[b] 4.7[c]
c-AlN			
$C_{11,c}$	$301+3.38P-0.003P^2$	$267+5.21P-0.077P^2$	304[a]
$C_{12,c}$	$166+3.09P-0.005P^2$	$141+4.26P-0.061P^2$	160[a]
$C_{44,c}$	$190+1.01P+0.005P^2$	$172+1.69P-0.015P^2$	193[a]
B_0	211	183	208[a]
B_0'	3.19	4.58	3.2,[b] 4.2[c]

[a]Reference 11.
[b]Reference 16.
[c]Reference 18.

$$C'_{44,M} = \frac{1}{6}(2C'_{11,c} - 2C'_{12,c} + 2C'_{44,c}) - \frac{2}{3}\frac{(C_{11,c} - C_{12,c} - 2C_{44,c})(C'_{11,c} - C'_{12,c} - 2C'_{44,c})}{(C_{11,c} - C_{12,c} + 4C_{44,c})} + \frac{1}{3}\frac{(C_{11,c} - C_{12,c} - 2C_{44,c})^2(C'_{11,c} - C'_{12,c} + 4C'_{44,c})}{(C_{11,c} - C_{12,c} + 4C_{44,c})^2}. \quad (8)$$

These linear coefficients together with the pressure-independent elastic constants for wurtzite materials obtained from Martin's transformation, $C'_{ij,M}$ and $C_{ij,M}$, respectively, are presented in Table IV. These values can be compared with values directly calculated for wurtzite structure (see Table II). As a measure of similarity, one can use the normalized root mean square (nrms) of the differences taken for each material. The values of nrms are included in Table IV. One can see that Martin's transformation for $C_{ij,M}$ gives the

TABLE IV. Elastic constants and their pressure derivatives for wurtzite nitrides, at ambient pressure, obtained using the Martin's transformation. The normalized root mean square (nrms) of the differences between results directly calculated and obtained using the Martin's transformation.

	$C_{11,M}$	$C'_{11,M}$	$C_{12,M}$	$C'_{12,M}$	$C_{13,M}$	$C'_{13,M}$	$C_{33,M}$	$C'_{33,M}$	$C_{44,M}$	$C'_{44,M}$	nrms(C_{ij})	nrms(C'_{ij})
wzGaN												
LDA	361	4.41	147	3.29	95	2.83	413	4.87	80	0.37	1.9%	10.4%
GGA	319	4.74	121	3.45	74	2.98	366	5.22	75	0.44	1.9%	9.2%
wzInN												
LDA	225	3.87	120	4.05	86	3.91	258	4.01	38	–0.11	3.9%	4.6%
GGA	186	4.94	90	4.38	61	4.0	215	5.32	35	0.16	3.9%	14.2%
wzAlN												
LDA	393	3.93	156	3.11	84	2.51	464	4.53	86	0.23	8.9%	9.5%
GGA	349	6.07	131	4.21	68	3.45	412	6.83	80	0.63	8.5%	19.5%

best results for GaN (nrms 1.9%) and the worst for AlN (nrms 8.5–8.9%). This agrees with the previous observation of Wright, who suggested that wurtzite GaN is most similar to zinc-blende, AlN is least similar, and InN is in between.[11] This tendency is not so clear, if one compares linear coefficients $C'_{ij,M}$ and C'_{ij}. Generally, the values of nrms are higher for the set of $C'_{ij,M}$ than for $C_{ij,M}$. It is particularly pronounced in the case of GaN. Moreover, considering the nrms for $C'_{ij,M}$, one observes significant differences in the values obtained by the LDA-DFT and GGA-DFT. For these reasons, we claim that, in contrary to the case of pressure-independent elastic constants, Martin's transformation is less suitable to obtain pressure-dependent elastic constants for wurtzite phase.

D. Pressure dependence of the Poisson coefficients

In the remainder of this section, we discuss the pressure dependence of the two-dimensional Poisson coefficient $\nu_{2D}(P)$, which relates the perpendicular strain component along the growth direction, e.g., ε_{zz}, to the lateral strain, e.g., ε_{xx}, resulting from the lattice constant mismatch between a nitride film and substrate. Of course, the Poisson coefficient is dependent on the growth direction. Here, we would like to discuss pressure dependence of the Poisson coefficient for the case of technologically most important growth directions, namely, [001] for cubic and [0001] for wurtzite phases of nitrides. Even if the direct comparison between these two nonequivalent crystallographic directions is impossible, we restrict the discussion to these two most important cases. For the [001] grown zinc-blende structure, the Poisson coefficient is defined as $\nu_{2D,c}(P)=2C_{12,c}(P)/C_{11,c}(P)$, whereas for [0001] wurtzite structure it takes the form $\nu_{2D}(P)=2C_{13}(P)/C_{33}(P)$.[1] In Table V, we show the values of the zero pressure Poisson coefficients $\nu_{2D}(0)$ together with their first pressure derivatives at ambient pressure ν'_{2D}. For [0001] grown wurtzite structure ν'_{2D} reads

$$\nu'_{2D}=\frac{2(C'_{13}C_{33}-C_{13}C'_{33})}{(C_{33})^2}. \tag{9}$$

The expression for ν'_{2D} in the case of [001] grown cubic layer can be obtained from Eq. (9) by substituting indices (13) and (33) with (12) and (11), respectively. Not surprisingly, the values of $\nu_{2D}(0)$ calculated in the present study are in good agreement with values reported in Ref. 11. However, in this section we would like to concentrate on ν'_{2D}. The knowledge of ν'_{2D} is important for determination of the pressure coefficient of the band gap, dE_G/dP, in strained layers. It turns out that dE_G/dP is significantly reduced by the term which is directly proportional to the product of ν'_{2D} and biaxial strain taken at ambient pressure.[1] This is true for both zinc-blende and wurtzite structures. Thus, one can regard ν'_{2D} as a good measure of the sensitivity of dE_G/dP to the biaxial strain in a material. On the other hand, the value of ν'_{2D} measures the influence of the nonlinear elasticity on dE_G/dP in strained material [in the linear second-order elastic theory $\nu'_{2D}=0$ by definition, see Eq. (9)]. From Table V, one can see that ν'_{2D} for [001] and [0001] strained zinc-blende and wurtzite phases are very similar for all studied nitrides. Thus, taking into account the nonlinear elasticity should reduce dE_G/dP in a similar way for the case of wurtzite and zinc-blende nitride strained structure considered here. It is interesting to note that ν'_{2D} is almost two times larger for InN than for GaN or AlN (see Table V). One can expect then the biaxial strain affects dE_G/dP in strained InN or InGaN layers more strongly than in strained GaN or AlGaN structures. We will discuss these points in the next section.

TABLE V. Two-dimensional Poisson coefficients and their first-order pressure derivatives for wurtzite (wz) and zinc-blende (c) nitrides.

	LDA—present results	GGA—present results	LDA[a]
c-GaN			
$\nu_{2D,c}(0)$	1.10	1.04	1.09
$\nu'_{2D,c}$	0.0083	0.0106	
c-InN			
$\nu_{2D,c}(0)$	1.36	1.26	1.34
$\nu'_{2D,c}$	0.0156	0.0199	
c-AlN			
$\nu_{2D,c}(0)$	1.10	1.056	1.05
$\nu'_{2D,c}$	0.0081	0.0113	
wz-GaN			
$\nu_{2D}(0)$	0.49	0.45	0.51
ν'_{2D}	0.0107	0.0100	
wz-InN			
$\nu_{2D}(0)$	0.81	0.74	0.82
ν'_{2D}	0.0203	0.0203	
wz-AlN			
$\nu_{2D}(0)$	0.60	0.576	0.58
ν'_{2D}	0.0120	0.0108	

[a]Reference 11.

III. PRESSURE COEFFICIENTS OF THE LIGHT EMISSION IN NITRIDE QWs

In this section, we examine how the pressure dependence of elastic constants influences the pressure coefficient of light emission, dE_E/dP, in wurtzite InGaN/GaN and GaN/AlGaN QWs grown along the c axis. In order to calculate dE_E/dP, one has to compute the changes of the highest hole and the lowest electron states in the QW with hydrostatic pressure. To reach this goal, we employed envelope function theory in the framework of multiband $k\cdot p$ method.[20] The $k\cdot p$ Hamiltonian includes changes of the band edges caused by strain in the system (through deformation potentials) and takes into account the electric fields induced by the differences in piezoelectric and spontaneous polarizations between well and barrier materials.

A. Strain in wurtzite heterostructures under external hydrostatic pressure

It is clear that the most important step in the calculation of dE_E/dP is the determination of strain tensor. Quantum well layers that are generally already strained owing to the lattice constants misfit at the ambient pressure are now subject to additional external hydrostatic pressure. In this situation, the strain tensor components are dependent on the applied hydrostatic pressure. To find this dependence, we use Hook's law,

$$\sigma_{\alpha\beta} = C_{\alpha\beta\chi\delta}(P)\varepsilon_{\chi\delta}, \tag{10}$$

where $\sigma_{\alpha\beta}$ is the stress tensor, $C_{\alpha\beta\chi\delta}(P)$ denotes the pressure-dependent fourth-order elastic stiffness tensor in the full tensor notation, and $\varepsilon_{\chi\delta}$ is the strain tensor. When external hydrostatic pressure, P_{out}, is applied to initially biaxially strained wurtzite QW structure, only diagonal elements of $\sigma_{\alpha\beta}$ and $\varepsilon_{\chi\delta}$ are nonzero and Eq. (10) reduces to the following matrix form (for simplicity, the Voigt notation for elastic constants is used here):

$$\begin{bmatrix} \sigma_{xx} \\ \sigma_{yy} \\ \sigma_{zz} \end{bmatrix} = \begin{bmatrix} F - P_{out} \\ F - P_{out} \\ -P_{out} \end{bmatrix} = \begin{bmatrix} C_{11}(P) & C_{12}(P) & C_{13}(P) \\ C_{12}(P) & C_{11}(P) & C_{13}(P) \\ C_{13}(P) & C_{13}(P) & C_{33}(P) \end{bmatrix} \begin{bmatrix} \varepsilon_{xx} \\ \varepsilon_{yy} \\ \varepsilon_{zz} \end{bmatrix}, \tag{11}$$

where F denotes the biaxial stress due to the lattice misfit between QW and barriers. From Eq. (11), one gets (*i*) the equality $\varepsilon_{xx}=\varepsilon_{yy}$ and (*ii*) the possibility to express ε_{zz} and F in terms of ε_{xx} and P_{out}:

$$\varepsilon_{zz} = -\frac{2C_{13}(P)}{C_{33}(P)}\varepsilon_{xx} - \frac{P_{out}}{C_{33}(P)}, \tag{12}$$

$$F = \left(C_{11}(P) + C_{12}(P) - 2\frac{[C_{13}(P)]^2}{C_{33}(P)} \right)\varepsilon_{xx} + P_{out}\left(1 - \frac{C_{13}(P)}{C_{33}(P)} \right). \tag{13}$$

Note that in the biaxially strained system the hydrostatic strain component is already present even in the absence of an external hydrostatic pressure. Therefore, the usual definition of hydrostatic pressure, $P=-\frac{1}{3}\text{Tr}(\sigma_{\alpha,\beta})$, leads to $P=P_{\text{out}}-\frac{2}{3}F$, which is obviously different than the externally applied pressure, P_{out}.

To complete the determination of the strain tensor components, one has to specify $\varepsilon_{xx}(P)$. This is, however, a highly nontrivial issue, since nitride-based epitaxial heterostructures are usually non-pseudomorphic. They are usually attached to a substrate through a non-pseudomorphic layer with high density of dislocations and of unknown elastic properties. Almost all high-pressure experiments for wurtzite nitride QWs were performed on structures grown on sapphire substrates,[6,20,21] where the QW structures exhibit various degree of relaxation. In order to provide quantitative comparison with experimental data and allow assessment of the nonlinear elasticity effects, one has to model this complicated strain situation. Generally, it has been commonly accepted that the interaction of QW structure with the substrate leads to effective lateral lattice constant dependent on pressure $a_s(P)$.[7,20,22] For example, following Ref. 20, for the heterostructures grown on sapphire substrates, one can estimate $a_s(P)$ as

$$a_s(P) = a_{0,br}(1 - P(S_{11,s} + S_{12,s} + S_{13,s})), \tag{14}$$

where $a_{0,br}$ is the equilibrium lattice constant of the barrier material and $S_{ij,s}$ $[(ij)=(11),(12),(13)]$, are the elements of elastic compliances tensor for sapphire.[23] Further, we follow this suggestion and assume additionally that the width of the QW is small in comparison to the widths of barriers. All this allows us to express ε_{xx} for the well and barrier regions as

$$\varepsilon_{xx,i}(P) = \frac{a_s(P) - a_{0,i}}{a_{0,i}}, \tag{15}$$

where i indicates the quantum well or barrier, and $a_{0,i}$ is the equilibrium lattice constant of the QW or barrier material.

B. Electric field in strained quantum wells

Having strain tensor components determined, in the second stage, we calculate the electric fields in the QW and barriers caused by spontaneous and piezoelectric polarizations. The nonvanishing z component of the total piezoelectric polarization in the [0001] QW structure is given as

$$P_{tot,i} = 2e_{31,i}\varepsilon_{xx,i} + e_{33,i}\varepsilon_{zz,i} + P_{spon,i}, \quad i = \text{QW,BAR}, \tag{16}$$

where $e_{31,i}$ and $e_{33,i}$ are the elements of piezoelectric tensor and $P_{spon,i}$ is the spontaneous polarization in the QW and the barrier (BAR).

Previously it has been shown that the piezoelectric constants e_{31} and e_{33} for a biaxially strained GaN and AlN layers differ from the values for the bulk.[24] Earlier works also suggested that this effect has to be considered in order to realistically describe the pressure light emission coefficient, dE_E/dP, in QWs.[6] Therefore, in the present study the change of the piezoelectric constants with biaxial strain has been fully taken into account (we use the results of Ref. 24) when calculating the piezoelectric polarization in strained quantum wells and barriers according to Eq. (16).

The values of the electric field along the growth direction in the QW (E_{QW}) and barrier (E_{BAR}) that results from the difference in the total electric polarizations in each region are given by simple formulas[25,26]

$$E_{QW} = \frac{2l_{BAR}(P_{tot,BAR} - P_{tot,QW})}{(2l_{BAR}\chi_{QW} + l_{QW}\chi_{BAR})}, \quad E_{BAR} = -\frac{l_{QW}}{2l_{BAR}}E_{QW}, \tag{17}$$

where l_{BAR}, l_{QW}, and χ_{BAR}, χ_{QW} are the thicknesses and the static dielectric constants for barrier and quantum well, respectively. We have assumed that the QW is surrounded on each side by the barrier of width l_{BAR} and that the potential on each side of the structure is equalized. If the barrier width is large enough in comparison to well width, this boundary condition is equivalent to the case with neutralizing external charges on the edges of the heterostructure.[26]

TABLE VI. Parameters used in the calculations of pressure coefficients of light emission.

Parameter	$Al_xGa_{(1-x)}N$	$In_xGa_{(1-x)}N$
a_0 (A)	$3.112x+3.189(1-x)$[a]	$3.545x+3.189(1-x)$[a]
E_g (eV)	$6.28x+3.44(1-x)-0.98x(1-x)$[b]	$0.8x+3.44(1-x)-2.5x(1-x)$[c]
Δ_1 (eV)	$-0.058x+0.022(1-x)$[b]	$0.041x+0.022(1-x)$[a,b]
$\Delta_2=\Delta_3$ (eV)	$-0.0068x+0.005(1-x)$[b]	$-0.001x+0.005(1-x)$[a,b]
m_z^c/m_0	$0.33x+0.2(1-x)$[b]	$0.12x+0.2(1-x)$[a,b]
A_1	$-3.95x-6.56(1-x)$[a]	$-8.21x-6.56(1-x)$[a]
A_2	$-0.27x-0.91(1-x)$[a]	$-0.68x-0.91(1-x)$[a]
A_3	$3.68x+5.65(1-x)$[a]	$7.57x+5.65(1-x)$[a]
A_4	$-1.84x-2.83(1-x)$[a]	$-5.23x-2.83(1-x)$[a]
A_5	$-1.95x-3.13(1-x)$[a]	$-5.11x-3.13(1-x)$[a]
A_6	$-2.91x-4.86(1-x)$[a]	$-2.91x-5.96(1-x)$[a]
a_c (eV)	$-4.5x-4.6(1-x)$[b]	$-3.5x-4.6(1-x)$[a,b]
D_1 (eV)	$-2.89x-1.7(1-x)$[b]	$0.55x+1.51(1-x)$[d]
D_2 (eV)	$4.89x+6.3(1-x)$[b]	$3.17x+5.21(1-x)$[d]
D_3 (eV)	$8.0x+7.78(1-x)$[b]	$4.92x+5.76(1-x)$[d]
D_4 (eV)	$-4.x-3.89(1-x)$[b]	$-1.79x+3.04(1-x)$[d]
D_5 (eV)	-4.0[a]	-4.0[a]
D_6 (eV)	-5.1[a]	-5.1[a]
e_{31}	$-0.53x-0.34(1-x)$[e]	$-0.41x-0.34(1-x)$[e]
e_{33}	$1.5x+0.67(1-x)$[e]	$0.81x+0.67(1-x)$[e]
P_{sp}	$-0.091x-0.034(1-x)+0.019x(1-x)$[e]	$-0.042x-0.034(1-x)+0.038x(1-x)$[e]
e'_{31}	$-3.5x-5.0(1-x)$[f]	-5.0[f]
e'_{33}	$-15x-16(1-x)$[f]	-16[f]
χ	$8.5x+10.4(1-x)$[g]	$15.3x+10.4(1-x)$[g]

[a]Reference 29.
[b]Reference 28.
[c]Reference 30.
[d]Reference 31.
[e]Reference 15.
[f]Reference 24.
[g]Reference 32.

In Eq. (17) the effect of screening by the residual background doping is not included.[25] More general analytic expressions for E_{QW}, which include this effect, have been proposed in Refs. 6 and 27. We do not use them in our calculations of dE_E/dP, since they introduce only an additional strain-independent term to the expression for E_{QW} [see Eq. (17)] and are not important for the calculation of dE_E/dP.

C. InGaN/GaN and GaN/AlGaN quantum wells—Results and discussion

Completing the setup of the $k\cdot p$ Hamiltonian, we are in the position to calculate the energies of the lowest electron and the highest hole states in the QWs. This is done by solving the effective mass equations for electrons and heavy holes separately. This procedure is justified, since the energy gap of quantum well material is sufficiently large in both considered GaN/AlGaN and InGaN/GaN QWs (with composition of indium below 20%). Since we are interested only in the maximum of the valence band energies at $k_\parallel=0$, the 6×6 $k\cdot p$ system of differential equations for six-component spinor of envelope functions reduces to a single equation for the heavy-hole component.[28] The shift of the band edges caused by strain is taken into account through the suitable deformation potentials. We assume that the deformation potentials do not depend on pressure. Previously we have found that for zinc-blende GaN and InN the hydrostatic deformation potentials are independent on P, whereas the shear deformation potentials show very weak pressure dependence and practically do not influence dE_G/dP in cubic InGaN/GaN QWs. Using the relations between the deformation potentials of the zinc-blende and wurtzite structure, one can also expect a weak dependence of the deformation potentials for wurtzite nitrides on hydrostatic pressure.[28]

The scheme described above provides the fundamental optical transition energies for QWs as a function of external pressure, $E_E(P_{out})$. These energies exhibit slight nonlinearity. To be consistent with experimental procedure,[6,20,21] the value of dE_E/dP is estimated from the linear fit to the E_E vs P_{out}. We use the above procedure to investigate the influence of nonlinear elasticity on dE_E/dP in wurtzite $In_{0.2}Ga_{0.8}N/GaN$ and $GaN/Al_{0.8}Ga_{0.2}N$ heterostructures with the QW widths lying between 1.8 and 5 nm, for which experimental values of dE_E/dP have been reported.[6,21] Table VI contains values of parameters used in the present calculations.

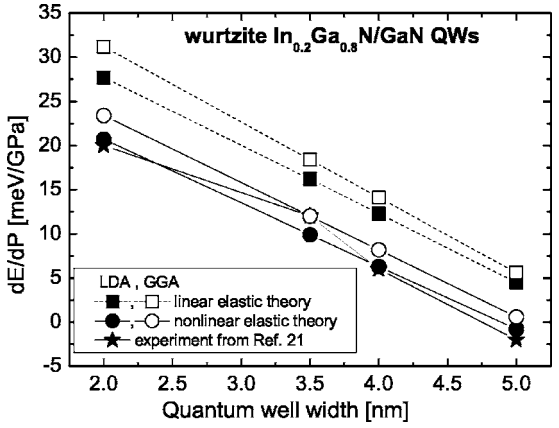

FIG. 4. Pressure coefficients of light emission energies (dE_E/dP) for wurtzite $In_{0.2}Ga_{0.8}N/GaN$ QWs as a function of quantum well width. Stars represent the experimental values of dE_E/dP taken from Ref. 21, squares correspond to theoretical values of dE_E/dP obtained using linear elastic theory, and circles correspond to dE_E/dP calculated using nonlinear elastic theory. Full and empty symbols represent values of dE_E/dP obtained using elastic constants calculated within LDA-DFT and GGA-DFT approaches, respectively. Solid and dashed lines are added to guide the eye.

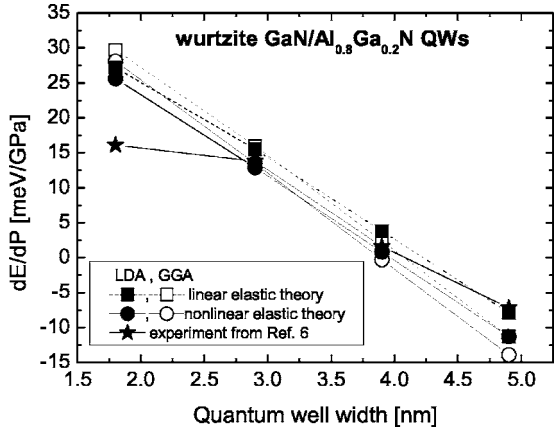

FIG. 5. Pressure coefficients of emission energies (dE_E/dP) for wurtzite $GaN/Al_{0.8}Ga_{0.2}N$ QWs as a function of QW width. Stars represent the experimental values of dE_E/dP, taken from Ref. 6. Squares correspond to theoretical values of dE_E/dP obtained using linear elastic theory. Circles correspond to dE_E/dP calculated using nonlinear elastic theory. Full and empty symbols represent values of dE_E/dP obtained using elastic constants calculated within LDA-DFT and GGA-DFT approaches, respectively. Solid and dashed lines are added to guide the eye.

In Fig. 4, we show theoretical values of dE_E/dP for wurtzite $In_{0.2}Ga_{0.8}N/GaN$ QWs as a function of QW width, obtained using linear [i.e., $C_{\alpha\beta}(P)=C_{\alpha\beta}(0)$] and nonlinear elastic theory within both LDA-DFT and GGA-DFT approaches. As can be seen in Fig. 4, the differences between LDA- and GGA-based results are rather small. Generally, the good agreement with experimental values of dE_E/dP is obtained in the case of nonlinear elastic theory, whereas the standard linear elastic theory leads to considerable quantitative discrepancies.

These results can be understood taking into account that the emission energy in a wurtzite quantum well (i.e., with polarization induced fields) may be expressed as

$$E_E = E_G + \Delta E_{cb} + \Delta E_{vb} - l_{QW}|eE_{QW}|, \tag{18}$$

where E_G is the bulk energy gap, ΔE_{cb} and ΔE_{vb} are confinement energies of electrons and holes, respectively, l_{QW} is the length of the QW, and $|eE_{QW}|$ is the electrostatic potential drop across the QW. Since the confinement energies are practically independent of the hydrostatic pressure, only the first and the fourth terms contribute to dE_E/dP. The expressions for dE_G/dP in the linear and nonlinear elastic theory differ by the term $\nu'_{2D}\cdot\varepsilon_{xx}(0)$, where ν'_{2D} is the pressure derivative of the two-dimensional Poisson coefficient and $\varepsilon_{xx}(0)$ is the biaxial strain at ambient pressure.[1,7] This leads to the pronounced differences in dE_E/dP (of order 5–8 meV/GPa for the $In_{0.2}Ga_{0.8}N/GaN$ heterostructures) calculated within the linear and non-linear elastic theory.

In both the linear and nonlinear elastic theory, a strong decrease of dE_E/dP with the QW width (l_{QW}) is observed. This effect has been attributed in the literature to the increase of polarization-induced electric field caused by external hydrostatic pressure[6] and is also confirmed by the present calculations. It can be easily understood taking into account that the confinement energies in Eq. (18) are practically independent on the hydrostatic pressure. Therefore, the dependence of the dE_E/dP on quantum well widths may come only from the fourth term in expression for E_E, i.e., from the pressure dependence of the electric field in QW.

Interestingly, the difference between dE_E/dP obtained within the linear elastic theory and the nonlinear one (hereafter, we indicated this difference as Δ) decreases with the QW width. Here, we would like to mention that, for cubic $In_{0.1}Ga_{0.9}N/GaN$ QWs, the difference in dE_E/dP obtained using linear and nonlinear elastic theory was about $\Delta=4$ meV/GPa and was independent on QW width.[7] Since the cubic heterostructures differ from the wurtzite ones by the lack of polarization-induced electric fields, the origin of the decrease of Δ with l_{QW} in wurtzite heterostructures may lie in the different values of dE_{QW}/dP_{out} (i.e., derivative of the electric field in QW with respect to the external pressure) as obtained in the linear and nonlinear elastic theory.

In Fig. 5, the dE_E/dP for the wurtzite $GaN/Al_{0.8}Ga_{0.2}N$ QWs are depicted as a function of QW width. Generally, we observe the similar qualitative behavior as in the case of $In_{0.2}Ga_{0.8}N/GaN$ QWs. However, the differences between values of dE_E/dP obtained with the nonlinear and linear elastic theory (Δ) are much smaller in $GaN/Al_{0.8}Ga_{0.2}N$ QWs than in the previously discussed $In_{0.2}Ga_{0.8}N/GaN$ heterostructures. Specifically, for 1.8 nm thick wurtzite $GaN/Al_{0.8}Ga_{0.2}N$ QWs, we have $\Delta=2$ meV/GPa, i.e., a factor of 4 smaller than in the $In_{0.2}Ga_{0.8}N/GaN$ QWs. To understand this large difference between values of Δ in both QWs, let us first notice that $\varepsilon_{xx}(0)$ is similar for $In_{0.2}Ga_{0.8}N/GaN$ QWs (2.2%) and $GaN/Al_{0.8}Ga_{0.2}N$ QWs (2%). Obviously ν'_{2D} is significantly higher for InN than for GaN (see Table II), which partially explains our results. However, we have additionally found out that there is an-

other reason for small value of Δ in $GaN/Al_{0.8}Ga_{0.2}N$ QWs. The small value of Δ in this case is related to the fact that in this structure the barriers were rather thin (5.2 nm) and the QW was initially unstrained. This is contrary to $In_{0.2}Ga_{0.8}N/GaN$ QWs where the barriers were thick and the QW was biaxially strained. To confirm this argument, we have performed additional calculation of dE_E/dP for the $GaN/Al_{0.8}Ga_{0.2}N$ heterostructures with thick barriers and strained QWs. In this case, Δ has increased almost by a factor of 2.

IV. GAN/AlN QUANTUM DOTS

As another example illustrating the role of nonlinear elasticity, we study elastic, piezoelectric, and optical properties of wurtzite GaN/AlN QDs with hexagonal pyramid shape.

In the first step, we calculate the distribution of strain in the quantum dot using linear and nonlinear elastic theory. Further, we calculate the distribution of the electric polarization and finally emission energies in QDs.

To obtain the strain distribution in the QD, we solve the boundary-value problem obtained from the integration of the equilibrium equation for stress tensor, $\mathrm{div}(\sigma_{\alpha\beta})=0$.[33] The stress-strain relation is described by Hook's law, as in Eq. (10), with the strain tensor that contains components corresponding to mismatch of lattice constants in QD and embedding materials. Since the stress distribution in a QD, $\sigma(x)$, has hydrostatic component, $P(x)=-\mathrm{Tr}[\sigma_{\alpha\beta}(x)]/3$, and the elastic constants in the nonlinear elasticity theory are dependent on pressure, the $\sigma(x)$ has been determined in a self-consistent manner. In these calculations the values of pressure-dependent elastic constants for wurtzite GaN (Table II) have been used.

In the second step, we calculate the piezoelectric polarization vector as

$$P_{tot,\alpha} = e_{\alpha\beta\chi}\varepsilon_{\beta\chi} + P_{sp,\alpha}, \tag{19}$$

where $e_{\alpha\beta\chi}$ denotes third-order piezoelectric tensor. In these calculations, we assume that the piezoelectric constants are strain independent. The electrostatic potential is obtained from the Poisson equation. Finally, we solve 8×8 $k\cdot p$ Hamiltonian for the wurtzite structure,[34] which has been symmetrized according to the standard procedure.[35]

All partial-differential equations in our approach are solved using the finite element method. Most of the parameters used in the model have been already listed in Table VI. The transformation formulas for the valence band parameters of 8×8 $k\cdot p$ Hamiltonian as well as the shear piezoelectric constants have been taken from Ref. 34.

We have performed calculation for a single GaN/AlN QD having the shape of a truncated hexagonal pyramid placed on 0.5 nm thick wetting layer. The height of the QD was 4 nm, the base diameter was 19.5 nm, and the angle between the base of the dot and a side wall was $\pi/6$. In Fig. 6, we present profiles of the built-in hydrostatic pressure and volumetric strain, $\varepsilon_{vol}(x)=\mathrm{Tr}[\hat{\varepsilon}(x)]$, taken from the center of the QDs, along z axis [0001], parallel to the direction of growth. One can see that the usage of the nonlinear elastic theory results in significant increase of local hydrostatic pressure P inside the QD by about 0.4 GPa. Simultaneously, the magnitude of ε_{vol} in the QD decreases when the nonlinear elasticity is used. In Table VII, we have listed differences between values of pressure, ΔP, volumetric strain, $\Delta\varepsilon_{vol}$, magnitude of the average z component of the built-in electric field, ΔE_z, and fundamental interband transition energy, ΔE_{c-v}, when the nonlinear and linear elastic theory have been used. Usage of nonlinear elasticity results in relative decrease of the absolute value of ε_{vol} by 7%. Interestingly, the magnitude of E_z increases by 0.1 MV/cm, compared to the results obtained using linear elastic theory. Both effects, i.e., decrease of ε_{vol} and increase of E_z, lead to substantial lowering of E_{c-v}

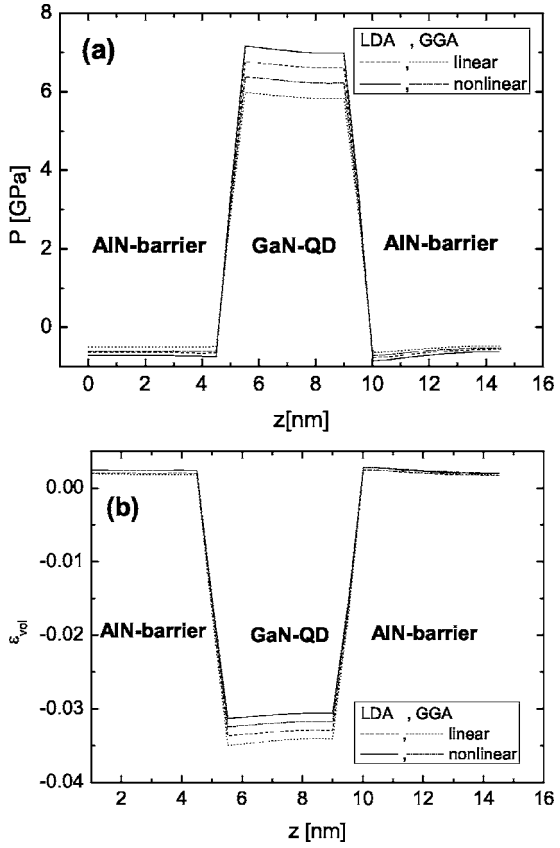

FIG. 6. Profiles of the built-in hydrostatic pressure (a) and volumetric strain (b) for a GaN/AlN QD, taken from the center of the QD along the z axis, i.e., parallel to the [0001] growth direction. Dotted and dashed lines show profiles obtained using linear elastic theory while dashed-dotted and solid lines correspond to results obtained using nonlinear elastic theory.

TABLE VII. Differences between results obtained using the nonlinear and linear elastic theory for a wurtzite GaN/AlN QD. Columns 2–5 contain differences in the built-in hydrostatic pressure, volumetric strain, average z component of the electric field, and fundamental band-to-band transition energy.

	ΔP	$\Delta\varepsilon_{vol}$	$\Delta\varepsilon_{vol}/\varepsilon_{vol(0)}$	ΔE_z (MV/cm)	ΔE_E (eV)
LDA-DFT	0.37	0.002 31	−7.0%	−0.10	0.070
GGA-DFT	0.40	0.002 37	−6.9%	−0.10	0.069

(70 meV in the calculated structure). These results clearly demonstrate that the nonlinear elasticity effects play a very important role in wurtzite hexagonal QDs and may not be ignored in any type of quantitative description.

V. CONCLUSIONS

We have studied the nonlinear elasticity effects for the case of InN, GaN, and AlN binary compounds. We have found that C_{11}, C_{12} in zinc-blende nitrides and C_{11}, C_{12}, C_{13}, C_{33} in wurtzite nitrides depend significantly on hydrostatic pressure. Much weaker dependences on pressure have been observed for C_{44} in both zinc-blende and wurtzite phases. Comparing elastic constants for wurtzite and zinc-blende nitrides, we have shown that the Martin's transformation is not suitable for application to pressure derivatives of elastic constants. The calculated values of the pressure derivative of the two-dimensional Poisson coefficients are by almost a factor of 2 higher for InN than for GaN or AlN. This explains why the nonlinear elasticity effects should modify dE_E/dP much stronger in strained InN or InGaN layers than in GaN, AlGaN, or AlN. Then, we have performed calculations of dE_E/dP in wurtzite nitride QWs, which confirmed predictions based on observed trends in bulk properties. We have determined that usage of nonlinear elastic theory results in reduction of dE_E/dP (as compared to the linear theory) about $\Delta = 8-5$ meV/GPa for wurtzite $In_{0.2}Ga_{0.8}N/GaN$ QWs and leads to the excellent agreement with experimental data. Finally, we have analyzed the influence of nonlinear elasticity on elastic, piezoelectric, and optical properties of wurtzite GaN/AlN QDs. It turns out that the nonlinear elasticity effects are crucial for quantitative description of energy spectra in hexagonal quantum dots.

ACKNOWLEDGMENTS

This work has been supported by the Polish State Committee for Scientific Research, Project No. 4T11F 008 25. The *ab initio* calculations of elastic constants have been performed using computer facilities at the Interdisciplinary Center for Mathematical and Computational Modeling of Warsaw University.

[1] M. D. Frogley, J. R. Downes, and D. J. Dunstan, Phys. Rev. B **62**, 13612 (2000).
[2] S. W. Ellaway and D. A. Faux, J. Appl. Phys. **92**, 3027 (2002).
[3] B. S. Ma, X. D. Wang, F. H. Su, Z. L. Fang, K. Ding, Z. C. Niu, and G. H. Li, J. Appl. Phys. **95**, 933 (2004).
[4] J.-W. Luo, S.-S. Li, J.-B. Xia, and L.-W. Wang, Phys. Rev. B **71**, 245315 (2005).
[5] R. Kato and J. Hama, J. Phys.: Condens. Matter **6**, 7617 (1994).
[6] G. Vaschenko, C. S. Menoni, D. Patel, C. N. Tome, B. Clausen, N. F. Gardner, J. Sun, W. Gotz, H. M. Ng, and A. Y. Cho, Phys. Status Solidi B **235**, 238 (2003).
[7] S. P. Łepkowski and J. A. Majewski, Solid State Commun. **131**, 763 (2004).
[8] W. E. Pickett, Comput. Phys. Rep. **9**, 117 (1989).
[9] G. Kresse and J. Furthmuller, Phys. Rev. B **54**, 11169 (1996).
[10] S. Bhagavantam, in *Crystal Symmetry and Physical Properties* (Academic Press, London, 1966), p. 147.
[11] A. F. Wright, J. Appl. Phys. **82**, 2833 (1997).
[12] D. M. Ceperley and B. J. Alder, Phys. Rev. Lett. **45**, 566 (1980); J. P. Perdew and A. Zunger, Phys. Rev. B **23**, 5048 (1981).
[13] J. P. Perdew, in *Electronic Structure of Solids '91*, edited by P. Ziesche and H. Eschrig (Akademie-Verlag, Berlin, 1991), p. 11.
[14] G. Kresse and D. Joubert, Phys. Rev. B **59**, 1758 (1999).
[15] A. Zoroddu, F. Bernardini, P. Ruggerone, and V. Fiorentini, Phys. Rev. B **64**, 045208 (2001).
[16] K. Kim, W. R. L. Lambrecht, and B. Segall, Phys. Rev. B **53**, 16310 (1996).
[17] For completeness, the previously published (Ref. 7) GGA results for cubic GaN and InN have been included in Fig. 3.
[18] S.-H. Wei and A. Zunger, Phys. Rev. B **60**, 5404 (1999).
[19] R. M. Martin, Phys. Rev. B **6**, 4546 (1972).
[20] S. P. Łepkowski, H. Teisseyre, T. Suski, P. Perlin, N. Grandjean, and J. Massies, Appl. Phys. Lett. **79**, 1483 (2001).
[21] P. Perlin, I. Gorczyca, T. Suski, P. Wisniewski, S. Łepkowski, N. E. Christensen, A. Svane, M. Hansen, S. P. DenBaars, B. Damilano, N. Grandjean, and J. Massie, Phys. Rev. B **64**, 115319 (2001).
[22] P. Perlin, L. Mattos, N. A. Shapiro, J. Kruger, W. S. Wong, T. Sands, N. W. Cheung, and E. R. Weber, J. Appl. Phys. **85**, 2385 (1999).
[23] F. Rosch and O. Weis, Z. Phys. B **25**, 102 (1976).
[24] K. Shimada, T. Sota, K. Suzuki, and H. Okumura, Jpn. J. Appl. Phys., Part 2 **37**, L1421 (1998).
[25] F. Bernardini and V. Fiorentini, Phys. Status Solidi B **216**, 391 (1999).
[26] J. A. Majewski, G. Zandler, and P. Vogl, J. Phys.: Condens. Matter **14**, 3511 (2002).
[27] J. L. Sanchez-Rojas, J. A. Garrido, and E. Munoz, Phys. Rev. B **61**, 2773 (2000).
[28] S.-H. Park and S.-L. Chuang, J. Appl. Phys. **87**, 353 (2000).
[29] I. Vurgaftman, J. R. Mayer, and L. R. Ram-Mohan, J. Appl. Phys. **89**, 5815 (2001).
[30] F. Bechstedt, J. Furthmuller, and J.-M. Wagner, Phys. Status Solidi C **0**, 1732 (2003).
[31] W. W Chow, A. F. Wright, A. Girndt, F. Janke, and S. W. Koch, Mater. Res. Soc. Symp. Proc. **468**, 487 (1997).
[32] H. Morkoc, *Nitride Semiconductors and Devices* (Springer-Verlag, New York, 1999).
[33] P. Dłużewski, G. Maciejewski, G. Jurczak, S. Kret, and J.-Y. Laval, Comput. Mater. Sci. **29**, 379 (2004).
[34] A. D. Andreev and E. P. O'Reilly, Phys. Rev. B **62**, 15851 (2000).
[35] G. A. Baraff and D. Gershoni, Phys. Rev. B **43**, 4011 (1991).